

Enrichment of Niobium and Titanium from Kaolin Using an Acid–Alkali Leaching Process



NING WANG, HANNIAN GU, HANJIE WEN, and SHIRONG LIU

Niobium is a strategic resource because it is useful in a wide number of applications and its global distribution is uneven. It has been reported that kaolin clay from the bottom of the Xuanwei Formation, the Late Permian sequences in southwest China, contains Nb. In this paper, the major, trace, and mineral compositions of kaolin clay were characterized using XRF, ICP-MS, and XRD. The results show that it is mainly composed of kaolinite, anatase, and rutile, with a chemical composition of Al₂O₃ 34.38 pct, SiO₂ 39.97 pct, TiO₂ 8.79 pct, Fe₂O₃ 3.24 pct, and Nb 491 μg/g. A process including calcination treatment and acid–alkali leaching with HCl and NaOH was employed to separate Al, Fe, and Si in a leaching solution and to enrich Nb and Ti in the residue. The experimental results indicated that the reaction temperature played a vital role for Al and Fe extractions from acid leaching, while the concentration of alkali was the key factor for Si extraction. Under the optimal conditions, the contents of Nb and Ti in the final product were 4280 μg/g and 80.5 pct, respectively.

<https://doi.org/10.1007/s11663-018-1405-6>

© The Minerals, Metals & Materials Society and ASM International 2018

I. INTRODUCTION

NIObIUM (Nb) is a strategic metal with a wide variety of uses, especially for ferroniobium alloys, superconducting magnets, electronic components, catalysts, *etc.*^[1–3] Nb usually exists as oxide minerals (such as pyrochlore, columbite, and fersmite) in the Earth's crust, and pyrochlore is the most important commercially exploitable niobium-containing mineral.^[4] Primary Nb deposits are associated with carbonatites and oversaturated alkaline-to-peralkaline granitoids, while secondary (or supergene) Nb deposits form in the zones of lateritic weathering above primary deposits.^[3,5] Traditional industrial methods to recover Nb from ores are either pyrometallurgical treatments or purification processes using hydrofluoric acid; additionally, hydrometallurgical processes of alkaline routes have been widely reported for the purification of Nb (and/or Ta) concentrates.^[6–10] In terms of the distribution of Nb, approximately 95 pct of Nb ore reserves were evaluated in

Brazil, and Brazil was also the world's leading niobium producer, with 90 pct of global production, followed by Canada with 9 pct.^[11] The increasing demand of industrial products that consume Nb, and the unbalanced distribution of Nb resources, have encouraged the exploitation and processing of new niobium resources.

The Late Permian sequences in southwest China are referred to as the Xuanwei Formation, and the lower part of this sequence is mainly composed of kaolinitic clay rocks in which niobium, rare earth elements, zirconium, and gallium have been evaluated as new polymetallic resources.^[12–14] The content of Nb in Nb-containing kaolin is mainly in the range of 200–600 μg/g and generally higher than that of some weathered crust Nb deposits in China (Nb₂O₅ 160 to 200 μg/g).^[15] However, it is a new type of Nb resource, and it is not precisely called “Nb ore” because of the lack of knowledge about its occurrence and the industrial process of beneficiation and metallurgy. So far, studies on this resource are still at an early stage,^[13] and previous works have focused on the geological and geochemical characteristics or genetic implications.^[12,13] The modes of occurrences of Nb have not been studied; moreover, research seldom refers to the extraction or enrichment of Nb resource from kaolin clay to give direction for prospective industrial applications.

Since the roasting process can transform kaolin to metakaolin, which is a nearly amorphous compound and highly soluble in acids,^[16] Nb and insoluble impurities, such as titanium oxides, can probably remain in the residue after leaching. In the current study, we characterized the Nb-containing kaolin clay from the Xuanwei Formation,

NING WANG and HANNIAN GU are with the Key Laboratory of High-temperature and High-pressure Study of the Earth's Interior, Institute of Geochemistry, Chinese Academy of Sciences, Guiyang, 550081, China. Contact e-mail: guhannian@vip.gyig.ac.cn HANJIE WEN is with the State Key Laboratory of Ore Deposit Geochemistry, Institute of Geochemistry, Chinese Academy of Sciences, Guiyang, 550081, China. SHIRONG LIU is with the State Key Laboratory of Environmental Geochemistry, Institute of Geochemistry, Chinese Academy of Sciences, Guiyang, 550081, China.

Manuscript submitted April 4, 2018.

and aimed to enrich Nb. After calcination, the kaolin sample was then executed by an acid leaching process and an alkali leaching process, which were effective for Al, Fe, and Si removal, while Nb and Ti were enriched in the residue. Conditions in the process, such as calcination temperature, leaching temperature, and amount of alkali, were also investigated in this study.

II. EXPERIMENT

A. Sample and Characterization Methods

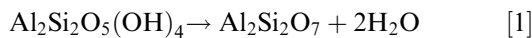
The kaolin clay was collected from the bottom of the Xuanwei Formation, Weining county, Guizhou, China. It was dried, ground, and homogenized for leaching experiments.

The main chemical compositions of the kaolin and residue samples were determined using XRF (PANalytical PW2424), and ICP-MS (Perkin Elmer Elan 9000) was used to analyze the trace elements concentration. The XRF analysis was determined in conjunction with a loss-on-ignition at 1000 °C. For ICP-MS determination, each sample was added to a lithium metaborate/lithium tetraborate flux, mixed well, and fused in a furnace at 1025 °C. The resulting melt was then cooled and dissolved in an acid mixture containing nitric, hydrochloric, and hydrofluoric acids. Finally, the solution was then analyzed by ICP-MS.

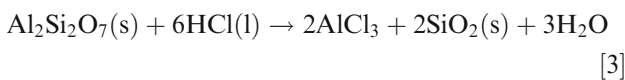
Powder X-ray diffraction measurements were performed using a PANalytical Empyrean diffractometer with Cu K α radiation. Each sample was prepared by compaction into a silicon sample holder, and a 2θ range between 5 and 70 deg was scanned. For SEM observation, samples were viewed with an FEI Scios scanning electron microscopy. TG and DSC analysis was performed on a thermal analyzer (Netzsch STA449 F3 Jupiter). Sample was investigated using air, and a temperature ramp rate of 10 °C min⁻¹ for heating from room temperature to 1200 °C was applied.

B. Acid-Alkali Leaching Process

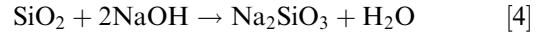
When temperatures higher than 550 °C are reached, kaolinite [Al₂Si₂O₅(OH)₄] dehydrates according to Eq. [1] and results in the formation of metakaolin [Al₂Si₂O₇], which is amorphous and active for acid-alkali leaching.^[16,17]



Al in metakaolin is reactive and could be leached by mineral acids with the following reactions, as shown in Eqs. [2] and [3]^[16]:



After Al was extracted, Si could be reactivated by using NaOH solution, as described in Eq. [4]. If alkali leaching was executed prior to Al acidic leaching, cementitious materials or zeolites might be obtained due to the presence of Al and impurities like Ca.^[18,19]



In this study, kaolin clay was calcined using a muffle furnace at different temperatures for 2 hours to obtain metakaolin. Subsequently, four group experiments were designed to investigate the effects of different parameters on Al, Fe, and Si extraction. Each calcined sample was added with the desired amount of acid to a beaker covered with plastic film. An electric heater (magnetic stirring apparatus) was used for heating to 100 °C, and a thermostatic water bath was used for heating to other temperatures. After filtration and washing with pure water 3 times, the acidic residue was leached using the desired amount of NaOH solution. The final product was obtained after filtration and washing. Specifically, different calcination temperatures of kaolin clay (from 500 °C to 850 °C) were evaluated in order to investigate its phase transformation. Reaction temperatures referred to the solid-liquid reaction for acid/alkali leaching processes, which were monitored using an electric heater/thermostatic water bath. The ranges of reaction temperatures for the acid and alkali leaching processes were designed as 20 °C to 100 °C and 40 °C to 80 °C, respectively. The concentration of NaOH was also selected as an operating parameter during the alkali leaching process to investigate the solubility of the product of Na₂SiO₃ in the leaching solution. Given that 2.5 mol/L NaOH was theoretically needed for Si leaching, 2 to 6 mol/L of NaOH solution was employed with a liquid-to-solid ratio of 5 mL:1 g.

GR grade hydrochloric acid (36.0 to 38.0 wt/vol pct, Sinopharm Chemical Reagent Co., Ltd) and sodium hydroxide (≥ 98.0 wt pct, Tianjin Kemiou Chemical Reagent Co., Ltd, China) were used for the leaching processes. The elements concentrations in the leaching solutions were determined by ICP-MS (Agilent 7700x) or ICP-OES (Varian VISTA).

The leaching ratio of a given element in this study was calculated according to the following equation:

$$\varepsilon(M, \text{pct}) = \frac{V \times C}{m \times w} \times 100 \quad [5]$$

where ε (M , pct) represents the leaching ratio of Al, Fe, or Si; V (L) is the total volume of acid or alkali leaching solution merged with washing solution; c (g/L) is the concentration of Al, Fe, or Si in the solution; m (g) is the weight of the original clay used; and w (pct) denotes the contents of Al, Fe, or Si in the clay sample.

Table I. Main Chemical Compositions of the Sample in this Study

Components	Al ₂ O ₃	SiO ₂	Fe ₂ O ₃	TiO ₂	BaO	CaO	Cr ₂ O ₃	K ₂ O	MgO	MnO	Na ₂ O	P ₂ O ₅	LOI
Content (wt pct)	34.38	39.97	3.24	8.79	0.02	0.03	0.03	0.05	0.10	0.02	0.05	0.09	13.01

Table II. Trace Elements Concentrations of the Kaolin Sample in this Study

Elements	Nb	Ta	V	Zr	Th	U	Sc	Y	La-Lu
μg/g	491	31.6	596	3480	85.8	15.25	75.3	38.1	281.4

III. RESULTS AND DISCUSSION

A. Chemical and Mineral Composition

Table I shows that Al₂O₃, SiO₂, TiO₂, and Fe₂O₃ occurred as the major constituents in kaolin clay. TiO₂ and Fe₂O₃ are common impurities in kaolin clays. In this study, the TiO₂ content was as high as 8.79 pct, much higher than other oxides (CaO, MgO, Na₂O, K₂O, and P₂O₅), which occurred as minor constituents. Nb and other trace elements are presented in Table II. It is worth mentioning that the 491 μg/g of Nb in the clay was even higher than that in the weathered crust Nb deposits in China. This meets the needs of the oxides of Nb and Ta, which should be not less than 160 to 200 μg/g, according to industry specifications.

Figure 1 shows TG and DSC curves of the kaolin clay used in this study. Thermal behavior from the TG analysis between 300 °C and 900 °C was used to quantify the content of OH groups,^[20] accompanying the transformation from kaolin to metakaolin.^[21] The main mass loss between 300 °C and 900 °C was 11.54 pct. The mass loss of the dehydroxylation process was overall less than the theoretical mass loss calculated from the mineral formulas (13.95 pct), due to the presence of impurities of Fe and Ti minerals in the sample. The DSC endothermic peak at 521.9 °C corresponded to the dehydroxylation process. It was reported that the DSC exothermic peak at 990.6 °C was related to the recrystallization of the amorphous phase and the formation of a mullite or spinel phase.^[21] In this study, an exothermic peak was observed at 989.0 °C, which was assigned to the recrystallization of amorphous phases.

Powder X-ray diffraction was performed (Figure 2) to identify the mineral phase composition of the kaolin clay sample. The mineralogical characterization was consistent with the major chemical analysis of the sample. In general, the mineral compositions of the kaolin clay were not complicated. Kaolinite (ICDD-PDF-2 code number 01-078-2109) and anatase (ICDD-PDF-2 code number 01-071-1168) can be matched well in the original kaolin sample, and kaolinite was the dominant mineral. The fingerprint peak of rutile (ICDD-PDF-2 code number 01-087-0710) can also be recognized, which indicates that high TiO₂ was in the

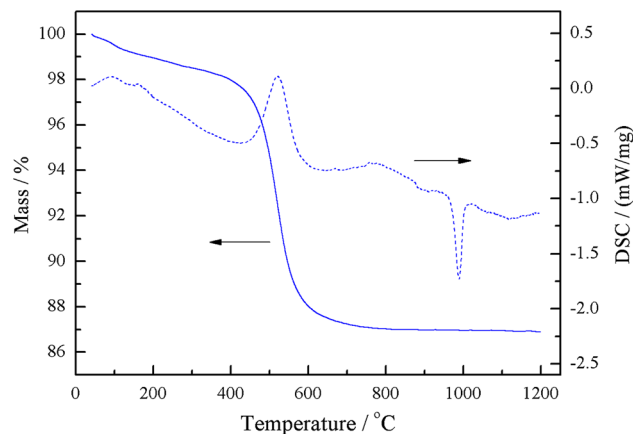


Fig. 1—TG and DSC curves of kaolin clay.

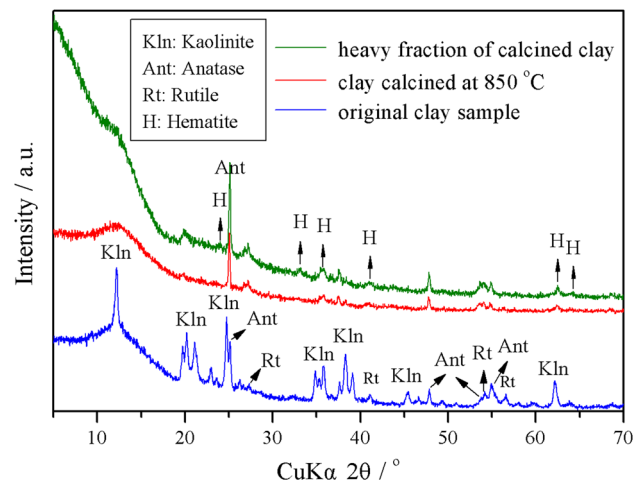


Fig. 2—XRD patterns of the original clay, calcined clay, and the heavy fraction.

form of both anatase and rutile. Titanium-bearing minerals and iron oxides occur ubiquitously as trace phases in kaolin clays^[22] due to the insolubility of Ti⁴⁺ and Fe³⁺.^[23] However, the fingerprints of iron-containing phases cannot be found in the diffraction patterns of the original kaolin clay in this study. To ascertain the iron-containing phases in the calcined clay sample, its

heavy fraction was separated by ultrasonic washing to remove the relatively light constituent. The samples of clay calcined at 850 °C and its heavy fraction are also shown in Figure 2. It is apparent that the reflections of the heavy fraction appeared in the weak peaks that matched those of hematite (ICDD-PDF-2 code number 00-024-0072) well. This indicates that hematite was one of the iron-containing phases in the clay sample. Other common impurities in kaolin,^[24] such as quartz, micas, illite, and montmorillonite, were not observed from the XRD pattern. This special mineral composition made it possible to separate Al and Si to enrich Nb and Ti.

B. Influence of the Calcination Temperature for Kaolin Converting and Al Leaching

Calcination of kaolinite at temperatures of > 550 °C promotes metakaolin ($\text{Al}_2\text{Si}_2\text{O}_7$) production *via* the dehydroxylation process.^[16] Metakaolin is an amorphous compound, in which Al is highly reactive to acid leaching. The kinetics of Al leaching from metakaolin derived from kaolin clays from different origins have been investigated using various mineral acids.^[16,25–28] Since the process of calcination is believed to increase kaolin clay's reactivity by affecting dehydration and transformation of the clay to an amorphous form,^[27] it is important to investigate the influence of the calcination temperature for kaolin dehydration. In this study, kaolin clay was calcined at temperatures of 500 °C, 550 °C, 650 °C, 750 °C, and 850 °C for 2 hours, and Figure 3 shows the changes in the XRD patterns of the raw kaolin and the converted products at various temperatures. From 550 °C onward, the phase of kaolin disappeared, converting to metakaolin, and only anatase and rutile can be observed in the patterns. This is in accordance with the literature findings reported before.^[16]

In this study, we aimed at obtaining a high leaching ratio of Al as well as Fe, for enriching Nb and Ti in the residue. The raw kaolin clay (only dried at 105 °C) and samples calcined at a series of different temperatures such as 500 °C, 550 °C, 650 °C, 750 °C, and 850 °C,

were used for experiments. For acid leaching process, experiments were performed at a reaction temperature of 100 °C for 1 hour, using HCl (1:2) as a leaching solution, with a liquid-to-solid ratio of 10 mL:1 g. The effects of calcination temperatures on the Al and Fe leaching ratios are shown in Figure 4. It can be seen that the sample dried only at 105 °C had a low leaching ratio of Al, approximately 3.9 pct. From 550 °C onward, Al started to be reactive in the acid solution, achieving a leaching ratio of 88 pct. These results can be ascribed to the conversion of metakaolin from the XRD analysis. The highest leaching ratio of Al accomplished was 98 pct, based on the sample obtained at 750 °C, which presented a similar trend reported by Ajemba and Onukwuli.^[27]

Fe exhibited much higher leaching ratios than those of Al for the raw kaolin clay (54 pct) and clay calcined at 500 °C (68 pct). It was reasonable that Fe was soluble in the raw kaolin clay and the sample calcined at 500 °C, for iron usually occurs as oxides in the clay and iron oxides are reactive to hot acid. With the increasing calcination temperatures, Fe also showed higher leaching ratios. We selected the sample calcined at 850 °C, as both Al and Fe had leaching ratios of more than 90 pct, which was good for subsequent Si leaching and Nb enrichment.

C. The Effect of Reaction Temperature for Al Leaching

Calcination temperature improved the reactivity of Al, and more than 90 pct of it was improved to be dissolved in the boiling HCl solution. To investigate the optimal reaction temperature for acid leaching, a water-bath heating method was used to obtain different temperatures for the Al dissolution process. The kaolin clay sample calcined at 850 °C was used for hydrochloric acid leaching using HCl (1:2) as a leaching solution, with a liquid-to-solid ratio of 10 mL:1 g, and each reaction lasted for 1 hour. Experimental results of Al and Fe leaching ratios are shown in Figure 5.

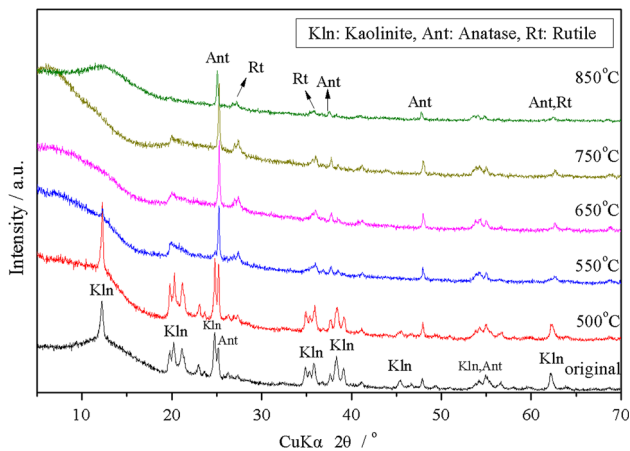


Fig. 3—XRD patterns of the original clay and calcined clay at different temperatures.

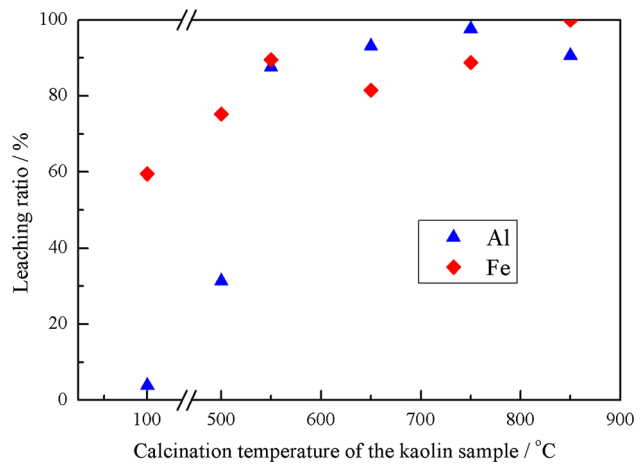


Fig. 4—Leaching ratios of Al and Fe using clay calcined at different temperatures. Condition of 100 °C for 1 h, using HCl (1:2) and liquid/solid of 10 mL:1 g.

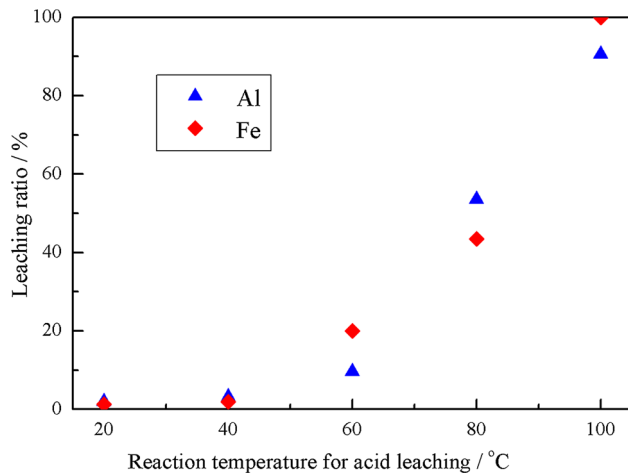


Fig. 5—Leaching ratios of Al and Fe with acid leaching at different reaction temperatures. Condition of sample calcined at 850 °C using HCl (1:2) and liquid/solid of 10 mL:1 g for 1 h.

As shown in Figure 5, with the increasing reaction temperature, both the leaching ratios of Al and Fe increased. As mentioned above, Fe in kaolin clay probably occurs as iron oxides, which do not readily react with acid at low temperatures. However, under the condition of 100 °C, 98 pct of the Fe in the sample was leached. In general, Al had a similar leaching trend in the solution in this study, and the optimal reaction temperature for Al leaching was 100 °C with a ratio of 91 pct.

D. The Effect of Alkali Concentration on Si Leaching

Since major elements, including Al and Fe, were leached using an HCl solution, Si became the major impurities for Nb and Ti enrichment. Subsequently, different concentrations of a NaOH solution were used to investigate the optimal amount of NaOH for extracting Si. Several kaolin clay samples calcined under 850 °C were used for acid leaching at 100 °C, and the precipitates were obtained after washing for alkali leaching. Precipitates were then processed using a liquid-to-solid ratio of 5 mL:1 g with different concentrations of NaOH as the leaching solution, and each reaction lasted 30 minutes at 70 °C. Afterward, the amounts of Si, Nb, and Ti in each filtrate were determined, and the data of the leaching ratios of Si, Nb, and Ti are shown in Figure 6.

Theoretically, if the NaOH added reacted with SiO₂ as given in Eq. [4], the concentration of NaOH could be calculated as approximately 2.5 mol/L when a liquid-to-solid ratio of 5 mL:1 g was used. As shown in Figure 6, the leaching ratios of Si using 2 and 3 mol/L were close, and 4 mol/L NaOH achieved nearly a 100 pct leaching ratio. However, higher concentrations made less Si enter into the solution. This was probably because of the surplus NaOH reacting with impurities and remnant Al, generating insoluble aluminosilicates. In the alkali leaching process, not only the leaching ratio of Si should be considered, but those of Nb and Ti should also be low in the alkali solution. In comparison

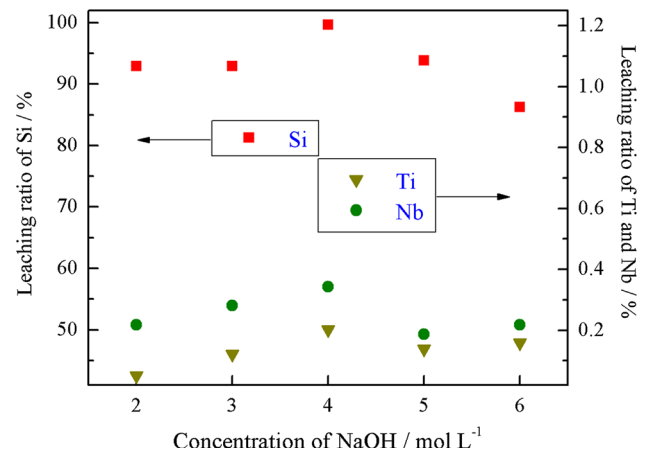


Fig. 6—Leaching ratios of Si with different NaOH concentrations in the alkali leaching process. Condition of reaction at 70 °C for 30 min with liquid/solid ratio of 5 mL:1 g.

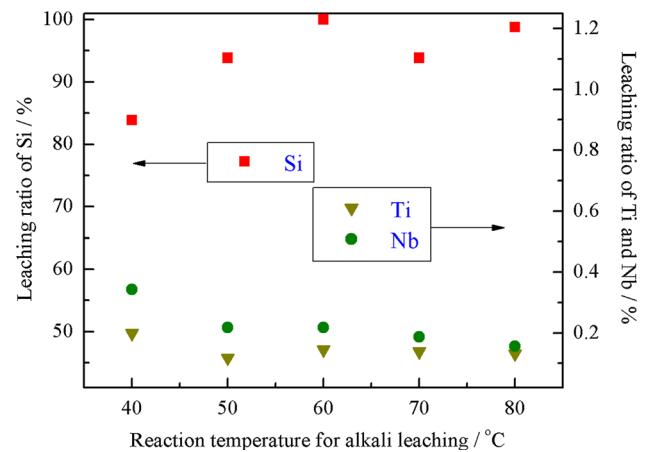


Fig. 7—Leaching ratios of Si with alkali leaching at different reaction temperatures. Condition of using 5 mol/L NaOH with liquid/solid ratio of 5 mL:1 g for 30 min.

with the acid leaching process, Nb and Ti tended to dissolve into the NaOH solution. In general, Nb and Ti had loss ratios (in the solution fraction) of 0.34 and 0.2 pct, respectively. However, using 5 mol/L NaOH, the Si leaching ratio was a little less than that when using 4 mol/L, and Nb and Ti dissolved less (0.19 pct for Nb and 0.14 pct for Ti) under the former condition. Therefore, 5 mol/L of NaOH solution was chosen as the optimal concentration for Si leaching.

E. The Effect of Reaction Temperature on Si Leaching

Reaction temperature for the NaOH process to extract Si was investigated based on the precipitates filtered from the acid leaching treatments. As Figure 7 illustrates, the leaching ratio of Si at 40 °C was 84 pct, and from 50 °C onward, it increased to 94 pct and seemed to get stabilized. During the alkali process, no more than 0.34 pct of Nb and 0.2 pct of Ti entered into the solution. It was observed that both the leaching ratios of Nb and Ti had a decreasing trend with the increasing reaction temperature.

F. Characterization of Final Product

Figure 8 shows the morphology of the final product (final residue) after the acid–alkali leaching process, under an optimal condition that was summarized as (a) calcination treatment: 850 °C for 2 hours; (b) acid leaching: HCl (1:2) and liquid/solid ratio of 10 mL:1 g, 100 °C for 1 hour; (c) alkali leaching: 5 mol/L NaOH with liquid/solid ratio of 5 mL:1 g, 60 °C for 30 minutes. In comparison to the original kaolin clay consisting of laminated kaolinite (seen in Figure 8(a)), the final product was composed of different morphologies of Ti minerals. It can be seen that the Ti minerals had a nanoscale size. The contents of Nb and Ti in the final product are listed in Table III, in comparison with original kaolin clay and kaolin calcined at 850 °C. The

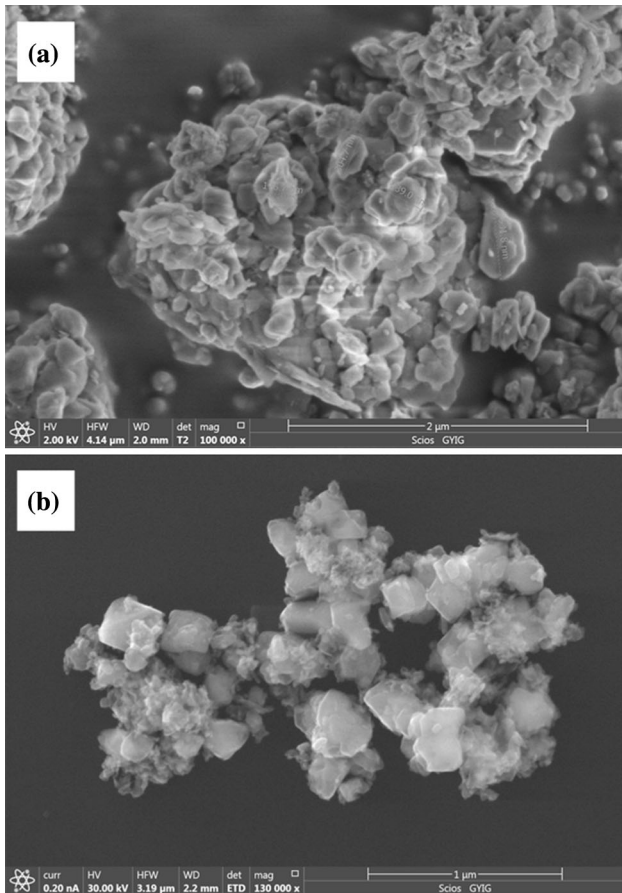


Fig. 8—SEM images of original clay (a) and the final product after the acid–alkali leaching process under optimal conditions (b).

result shows that the contents of Nb and Ti in the final product were 0.428 and 80.5 pct, respectively, achieving approximately nine times more than that in the original kaolin clay. It is also calculated that the recovery yields of Nb(Ta) and Ti were approximately 80 ± 5 pct. The calcined clay was lightly enriched with Nb and Ti due to the mass loss during the dehydroxylation process, while in the final product, Nb and Ti contents remarkably increased corresponding to the leaching of Al, Si, and Fe. Table III also provides the enrichment factor obtained from the ratio of concentrations of Nb(Ta) and Ti in final product to those in original clay. These data stressed that the process of calcination and acid–alkali leaching for kaolin clay was effective for enrichment of Nb and Ti.

Figure 9 shows the XRD patterns of the final product from the acid–alkali leaching process, as well as the intermediate product and original material. The peaks corresponding to kaolinite disappeared, and the relative intensity of Ti minerals peaks became stronger with the treatment of acid leaching and alkali leaching because aluminum and silicon were dissolved. In addition, “rutile, Nb-rich” (ICDD-PDF-2 code number 00-016-0934), with a formula of $(\text{Ti, Nb, Ta, Fe})\text{O}_2$ can be identified in the pattern of the final product. It is hard to know the concentration of Nb in the mineral of “rutile, Nb-rich” from the current study. However, from this point of view, we concluded that the final product was enriched with Ti-containing minerals, and Nb

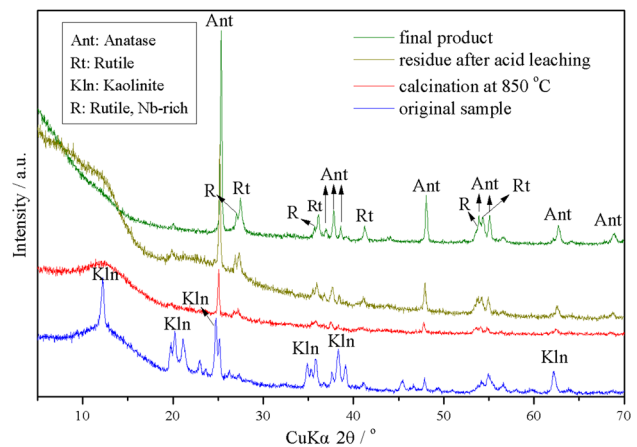


Fig. 9—XRD patterns comparisons of original clay, calcined clay, residue after acid leaching and the final product.

Table III. Contents of Nb, Ta and TiO_2 in Samples of Different Stages

Elements	Content wt pct			Enrichment factor
	Kaolin Clay	Calcined Clay	Residue	
Nb	0.0491	0.0534	0.428	8.72
Ta	0.0032	—	0.030	9.38
TiO_2	8.79	9.84	80.5	9.16

— unanalyzed.

(together with Ta and some other metals) might be within the lattice of Ti minerals as a form of isomorphism.

Niobium would be transferred into V-Cu residues as impurity during the process of chlorination and purification of TiCl_4 .^[29] Since the final product in this study contains up to 0.428 pct Nb and 80.5 pct Ti, it would be of potential interest as a raw material for titanium metallurgy and be of great value to withdraw Nb as resources during the process.

IV. CONCLUSIONS

The major chemical compositions of the kaolin clay from Xuanwei Formation were Al_2O_3 , SiO_2 , TiO_2 , and Fe_2O_3 . Meanwhile, the kaolin clay contained 491 $\mu\text{g/g}$ of niobium, which was higher than the industrial grade and could be exploited if the cost was economically viable. Kaolinite, anatase, and rutile existed in kaolin clay as the main mineral phases, and no other mineral phase was found.

A process including acid-alkali leaching with HCl and NaOH following calcination was employed to separate Al, Fe, and Si in the solution, and remarkably enriched Nb and Ti in the residue. The experimental results indicate that the reaction temperature played a vital role for Al and Fe extractions using acid, while for Si extraction, the concentration of alkali was the key factor. The optimal conditions to achieve Al and Fe extractions of 91 and 98 pct, respectively, were as follows: 1:2 HCl, reaction temperature of 100 °C, liquid-to-solid ratio of 10:1 v/w, and reaction time of 1 hour. To achieve an Si extraction of 94 pct and a Nb loss ratio of 0.19 pct, the optimal conditions for alkali leaching were 5 M HCl, a liquid-to-solid ratio of 5:1 v/w, and a reaction time of 30 minutes. Finally, the contents of Nb and Ti in the residue were 0.428 and 80.5 pct, respectively, achieving approximately nine times more than that from the original kaolin clay.

ACKNOWLEDGMENTS

The work was financially supported by the National Key Research and Development Program of China (2017YFC0602503), the National Natural Science Foundation of China (Grant No. 41402039), the Guizhou Scientific and Technological Innovation Team (2017-5657), the Guizhou Provincial Science and Technology Foundation (No. [2016]1155), and the Guizhou Science and Technology Major Program (No. [2016]3015). The authors are grateful to Dr Y. Meng

and Dr Z. Qin for their help with their analytical test and examination.

REFERENCES

1. E.L.S. Ngee, Y. Gao, X. Chen, T.M. Lee, Z. Hu, D. Zhao, and N. Yan: *Ind. Eng. Chem. Res.*, 2014, vol. 53, pp. 14225–33.
2. R.H. Mitchell: *Ore Geol. Rev.*, 2015, vol. 64, pp. 626–41.
3. G.J.-P. Deblonde, A. Chagnes, V. Weigel, and G. Cote: *Hydrometallurgy*, 2016, vol. 165, pp. 345–50.
4. X. Ni, M. Parrent, M. Cao, L. Huang, A. Bouajila, and Q. Liu: *Miner. Eng.*, 2012, vols. 36–38, pp. 111–18.
5. D. Beltrami, G.J.-P. Deblonde, S. Bélair, and V. Weigel: *Hydrometallurgy*, 2015, vol. 157, pp. 356–62.
6. G.J.-P. Deblonde, A. Chagnes, S. Bélair, and G. Cote: *Hydrometallurgy*, 2015, vol. 156, pp. 99–106.
7. G.J.-P. Deblonde, V. Weigel, Q. Bellier, R. Houdard, F. Delvallée, S. Bélair, and D. Beltrami: *Sep. Purif. Technol.*, 2016, vol. 162, pp. 180–87.
8. X. Wang, S. Zheng, H. Xu, and Y. Zhang: *Hydrometallurgy*, 2009, vol. 98, pp. 219–23.
9. H. Zhou, D. Yi, Y. Zhang, and S. Zheng: *Hydrometallurgy*, 2005, vol. 80, pp. 126–31.
10. H. Zhou, S. Zheng, and Y. Zhang: *Hydrometallurgy*, 2005, vol. 80, pp. 83–89.
11. USGS: 2014 Minerals Yearbook, 2016, April, 52, pp. 1–12.
12. S. Dai, Y. Zhou, M. Zhang, X. Wang, J. Wang, X. Song, Y. Jiang, Y. Luo, Z. Song, Z. Yang, and D. Ren: *Int. J. Coal Geol.*, 2010, vol. 83, pp. 55–63.
13. L. Zhou, Z. Zhang, and Y. Li: *J. Asian Earth Sci.*, 2013, vol. 73, pp. 184–98.
14. Z. Zhang, G. Zheng, Y. Takahashi, C. Wu, C. Zheng, J. Yao, and C. Xiao: *Ore Geol. Rev.*, 2016, vol. 72, pp. 191–212.
15. DZ/T 0203-2002, 2002. Geology Mineral Industry Standard of P.R. China: Specifications for Rare Metal Mineral Exploration. Geological Press, Beijing. (in Chinese).
16. P.E.A. Lima, R.S. Angélica, and R.F. Neves: *Clay Miner.*, 2017, vol. 52, pp. 75–82.
17. H.G. Dill: *Earth-Sci. Rev.*, 2016, vol. 161, pp. 16–129.
18. N.E. Gordina, V. Yu, Y.N. Prokofev, N.V. Kul'pina, S.I. Petuhova, and O.E. Hmylova: *Ultrason. Sonochem.*, 2016, vol. 33, pp. 210–19.
19. K. Wianglor, S. Sinthupinyo, M. Piyaworapaiboon, and A. Chaipanich: *Appl. Clay Sci.*, 2017, vol. 141, pp. 272–79.
20. V.A. Drits, A. Derkowski, B.A. Sakharov, and B.B. Zviagina: *Am. Miner.*, 2016, vol. 101, pp. 2331–46.
21. Y. Liu, S. Lei, M. Lin, Y. Li, Z. Ye, and F. Fan: *Appl. Clay Sci.*, 2017, vol. 143, pp. 159–67.
22. P.A. Schroeder and G. Erickson: *Elements*, 2014, vol. 10, pp. 177–82.
23. L.B. Railsback: *Geology*, 2003, vol. 31, pp. 737–40.
24. C. Detellier and R.A. Schoonheydt: *Elements*, 2014, vol. 10, pp. 201–06.
25. R.O. Ajemba and O.D. Onukwuli: *J. Energy Trends Eng. Appl. Sci.*, 2012, vol. 3, pp. 448–54.
26. M.R. Altiokka, H. Akalin, N. Melek, and S. Akyalçin: *Ind. Eng. Chem. Res.*, 2010, vol. 49, pp. 12379–82.
27. M.R. Altiokka and H.L. Hoşgün: *Hydrometallurgy*, 2003, vol. 68, pp. 77–81.
28. P.E.A. Lima, R.S. Angélica, and R.F. Neves: *Appl. Clay Sci.*, 2014, vols. 88–89, pp. 159–62.
29. H. Gu, N. Wang, and Y. Yang: *Waste Biomass Valori.*, 2017, <https://doi.org/10.1007/s12649-017-0112-x>.